X-550-70-92
PREPRINT

NASA TM X-63881

RADIATION PRESSURE EFFECTS ON THE ACCELERATION OF HIGH ALTITUDE BALLOON SATELLITES

DAVID E. SMITH
KENNETH H. FEA

MARCH 1970

GODDARD SPACE FLIGHT CENTER
GREENBELT, MARYLAND

X-550-70-92

PREPRINT

RADIATION PRESSURE EFFECTS ON THE ACCELERATION OF HIGH ALTITUDE BALLOON SATELLITES

David E. Smith

Mission and Trajectory Analysis Division

Kenneth H. Fea

University of London

England

March 1970

GODDARD SPACE FLIGHT CENTER

Greenbelt, Maryland

PRECEDING PAGE BLANK NOT FILMED.

RADIATION PRESSURE EFFECTS ON THE ACCELERATION OF HIGH ALTITUDE BALLOON SATELLITES

David E. Smith

Mission and Trajectory Analysis Division

Kenneth H. Fea

University of London

England

ABSTRACT

Previous studies of the orbital accelerations of the high altitude balloon satellites, Pageos and 1963-30D have shown the existence of perturbations that appear to be related to solar radiation pressure but of unknown mechanism. The normal method of computing the radiation perturbations assumes the effective shape of the spacecraft to be spherical but in the present paper an investigation is undertaken to assess the perturbations that may arise when the satellite has an ellipsoidal shape and the radiation scattered by the spacecraft is no longer symmetric about the line joining the satellite and the sun. Consideration is given to both diffuse and specular reflection. The study indicates that a slowly precessing rotation axis might explain the anomalous accelerations found in the earlier studies.

PRECEDING PAGE BLANK NOT FILMED.

CONTENTS

	Page
ABSTRACT	iii
INTRODUCTION	1
INCIDENT AND REFLECTED RADIATION	2
PERTURBATIONS OF THE SEMI-MAJOR AXIS	8
EXAMPLE	12
CONCLUSIONS	14
REFERENCES	15

RADIATION PRESSURE EFFECTS ON THE ACCELERATION OF HIGH ALTITUDE BALLOON SATELLITES

INTRODUCTION

Recent studies by Fea (Reference 1) and Fea and Smith (Reference 2) have shown the existence of an unexplained perturbation of the acceleration of two high altitude spacecraft. Both the spacecraft are balloon satellites of large area to mass ratio and in References 1 and 2 it was suggested that the unexplained acceleration might be associated with or caused by solar radiation pressure.

Figures 1 and 2, taken from References 1 and 2, show the predicted and observed accelerations of Pageos (1966-56A) and Dash 2 (1963-30D). The difference between the computed and observed accelerations is the unexplained perturbation. Inspection of Figures 1 and 2 indicates several important features of the perturbation. Firstly, the perturbation is periodic; secondly, the perturbation is only present when part of the orbit is in shadow (or the amplitude is considerably reduced), thirdly, the amplitude of the perturbation is comparable to the perturbation by solar radiation pressure, and fourthly, the period of the perturbation is decreasing.

There is evidence (References 3 and 4) that one of the satellites showing this anomalous acceleration (Pageos) is no longer spherical and that it is probably shaped like a prolate spheroid. If this is true, the major assumption made in calculating the radiation pressure perturbations, namely, that the solar radiation scattered by the satellite is symmetrical about the satellite-sun line, no longer holds. In such circumstances it must be expected that additional perturbations of the orbit will arise.

In the present paper the perturbations to the semi-major axis of the orbit of a satellite having the shape of a prolate spheroid are developed. The satellite is assumed to be rotating about the major or a minor axis of the spheroid with a period considerably less than the period of revolution of the satellite about the Earth. Sunlight scattered by the satellite is assumed to be reflected both diffusely (according to Lambert's law) and specularly.

INCIDENT AND REFLECTED RADIATION

Let the satellite have the shape of a prolate spheroid whose surface is described by the equation

$$\frac{(x^2 + y^2)}{b_0^2} + \frac{z^2}{a_0^2} = 1 \qquad (1)$$

where a_0 is the semi-major axis (polar radius)

b_0 is the semi-minor axis (equatorial radius)

and the origin of the coordinate system is at the center of the spheroid with the z - axis corresponding to the polar radius and the x and y axes lying in the equator. Let the angle between the z - axis and the sun be θ, then the shape of the cross-section normal to the sun-satellite line is an ellipse of area $A(\theta)$ where

$$A(\theta) = \pi b_0 d \qquad (2)$$

where

$$\frac{1}{d^2} = \frac{\sin^2\theta}{a_0{}^2} + \frac{\cos^2\theta}{b_0^2} \tag{3}$$

If the satellite is spinning about its major axis then the average cross-sectional area over one revolution of the satellite is $A(\theta)$ and the incident solar flux, F_I, is given by

$$F_I = A(\theta)\,\frac{S}{c} \tag{4}$$

where S is the solar constant in erg cm^{-2} sec^{-1}

c is the velocity of light in cm sec^{-1}

If, however, the satellite is rotating about a minor axis making an angle θ' with the sun-satellite line then $A(\theta)$ is a function of time and we need its average value.

Let $A(\theta')$ be the average value of $A(\theta)$ then

$$A(\theta') = \frac{1}{2\pi}\int_0^{2\pi} A(\theta)\,d\omega \tag{5}$$

where ω is the angle between the sun-rotation axis plane and the major axis of the satellite-rotation axis plane (see Figure 3). From Figure 3 we obtain

$$\cos\theta = \sin\theta'\,\cos\omega \tag{6}$$

and hence

$$A(\theta') = \frac{b_0}{2} \int_0^{2\pi} [d] \; d\omega \tag{7}$$

Substituting for d from Equation 3 and for θ from Equation 6 leads to

$$A(\theta') = \frac{a_0 \, b_0}{2} \int_0^{2\pi} \frac{d\omega}{(1 - k \cos^2 \omega)^{1/2}} \tag{8}$$

where

$$k = \left(1 - \frac{a_0^2}{b_0^2}\right) \sin^2 \theta' \tag{9}$$

The solution to Equation (8) is a hypergeometric function, and can be written as

$$A(\theta') = \pi \, a_0 \, b_0 \; F\left(\frac{1}{2}, \frac{1}{2}, 1, k\right) \tag{10}$$

where

$$F\left(\frac{1}{2}, \frac{1}{2}, 1, k\right) = \sum_{n=0}^{\infty} \left[\frac{(2n)!}{2^{2n} (n!)^2}\right]^2 k^n \tag{11}$$

The average incident solar flux on a prolate spheroid rotating about a minor axis can therefore be written

$$F_I = A(\theta') \frac{S}{c} \tag{12}$$

If the satellite were spherical the solar radiation that is reflected specularly would be distributed evenly over the entire unit sphere surrounding the satellite. If, however, the satellite is prolate or oblate there will be a direction about which the specular reflection will be largely symmetric and which will be the effective direction of any forces arising from the specular reflection. This direction will, for reasons of symmetry, lie in the plane containing the rotation axis of the satellite and the sun. We now make the first major assumption; that the effective direction of reflection of the specular flux is determined by Snell's law on the incident ray that passes through the center of the satellite (see Figure 4). We also make the assumption that the magnitude of the flux reflected in this direction approximates to that which would be reflected by a sphere of surface area equal to that of the spheroid. Hence the specularly reflected flux, E_s, can be written

$$E_s = \alpha_s \frac{\bar{A}}{4\pi}\left(\frac{S}{c}\right) \tag{13}$$

where

$$\left.\begin{aligned} \bar{A} &= A(\theta) \quad \text{for rotation about the major axis} \\ \bar{A} &= A(\theta') \quad \text{for rotation about a minor axis} \end{aligned}\right\} \tag{14}$$

and α_s is the specular albedo of the satellite.

The assumption concerning the direction of the reflection holds for $\theta = 0$, $\pi/2$ and π (also θ'), and for $0 < \theta \lesssim \pi/2$ and $\pi/2 < \theta < \pi$ the direction of reflection is moved towards the minor axis direction as indicated by Snell's law. Thus the assumption is considered adequate for the present study.

Similar arguments can be applied to the magnitude of the reflection; the magnitude of the flux for $\theta = 0$ is probably overestimated but underestimated for $\theta = \pi/2$. An exact formulation of the magnitude and effective direction of the specular reflection is extremely complex and is, at present, believed to be unnecessary for the present study.

Diffusely reflected radiation is normally symmetric about the normal to the surface and this is the assumption made here (see Figure 4). The satellite is assumed to be a uniformly diffuse reflector (Lambert's law) and for the purposes of calculating the dependence of the magnitude on the phase (not the size) the satellite is assumed to be spherical.

In Reference 5 the author has derived an expression for diffusely reflected radiation falling on a unit area distant r from the satellite. By putting $r = 1$ this expression may be used to give the flux (E_D) reflected diffusely in the direction of the normal to the surface on the incident ray that passes through the center of the satellite. We therefore have

$$E_D = \frac{2}{3} \alpha_D \frac{\bar{A}}{\pi^2} \left(\frac{S}{c}\right) \left[(\pi - \epsilon) \cos \epsilon + \sin \epsilon\right] \quad (15)$$

where a_D is the diffuse albedo of the satellite,

$$\epsilon = \frac{\pi}{2} - (\theta + \phi)$$

and (16)

$$\tan \phi = \left(\frac{b_0^2}{a_0^2}\right) \Big/ \tan \theta$$

for rotation about the major axis, or where

$$\epsilon = \theta' - \phi'$$

and (17)

$$\tan \phi' = \left(\frac{b_0^2}{a_0^2}\right) \tan \theta'$$

for rotation about a minor axis.

For convenience, we summarize the directions of the incident and emitted fluxes as follows:

(a) The incident flux, F_I, is directed radially from the sun through the center of the satellite; its magnitude is given by Equations 4 or 12;

(b) The specularly reflected flux, E_s, lies in the plane containing the sun and axis of rotation of the spacecraft and makes an angle 2ϵ with the incident ray through the center of the satellite; the magnitude is given by Equation 13,

(c) The diffusely reflected flux, E_D, lies in the plane containing the sun and the axis of rotation of the spacecraft and makes an angle ϵ with the incident ray through the center of the satellite, the magnitude is given by Equation 15.

As a check on the effect of the approximations we have made we can integrate the specular and diffuse fluxes (Equations 13 and 15) over the entire unit sphere. This integration leads to

$$\text{total reflected flux} = \bar{A}\left(\frac{S}{c}\right)(\alpha_s + \alpha_D) \tag{18}$$

If $(\alpha_s + \alpha_D) = 1$, then the total reflected flux is equal to the total incident flux (Equation 4) which means that the approximations (on average) only affect the relative magnitudes of the specular and diffuse components and not the total flux. If $(\alpha_s + \alpha_D) < 1$, the satellite is absorbing some of the incident radiation and implies we are making the additional assumption that when the satellite re-emits the absorbed radiation it does so isotropically so that there is no change in momentum of the satellite.

PERTURBATIONS OF THE SEMI-MAJOR AXIS

The semi-major axis is a measure of the energy of the orbit and hence the perturbations to the semi-major axis are equal to the work done by the forces of radiation pressure on the satellite. The perturbations to the semi-major axis can therefore be written as (Reference 6)

$$\Delta a = \frac{2F}{n^2 a m} \left[r \cos \phi \right]_{\text{shadow exit}}^{\text{shadow entry}} \qquad (19)$$

where

Δa is the change in the semi-major axis per revolution

F is the flux of radiation (F is negative)

n is the mean motion

a is the semi-major axis

m is the mass of the satellite

r is the geocentric radial distance of the satellite

ϕ is the angle between the sun and the satellite (see Figure 5)

Applying equation 19 to the incident and reflected fluxes already derived we obtain

$$\Delta a = - \frac{2}{n^2 a m} \left[r \left\{ F_I \cos \phi_0 + E_D \cos \phi_1 + E_s \cos \phi_2 \right\} \right]_{\text{shadow exit}}^{\text{shadow entry}} \qquad (20)$$

where ϕ_0, ϕ_1 and ϕ_2 are the angles between the satellite and the incident, diffuse and specularly reflected flux directions (see Figure 5).

Subsequently, we shall want to allow the spin axis to precess about another axis so we shall assume we know the direction of the precession axis $(\bar{\omega}, \bar{\theta})$

with respect to the sun (see Figure 5), the position of the sun (α, δ), the position of the spin axis (ω_s,θ_s) with respect to the precesson axis (see Figure 5) and the position of the satellite (α_0, δ_0).

With the aid of Figure 5 we can derive the right ascension ($\bar{\alpha}$) and declination ($\bar{\delta}$) of the precession axis from

$$\begin{aligned} \sin\bar{\delta} &= \cos\bar{\theta}\sin\delta + \sin\bar{\theta}\cos\delta\cos\bar{\omega} \\ \sin(\bar{\alpha} - \alpha) &= \frac{\sin\bar{\theta}\sin\bar{\omega}}{\cos\bar{\delta}} \end{aligned} \tag{21}$$

and the spin axis (α_s, δ_s) from

$$\begin{aligned} \sin\delta_s &= \cos\theta_s\sin\bar{\delta} + \sin\bar{\theta}_s\cos\bar{\delta}\cos\omega_s \\ \sin(\alpha_s - \bar{\alpha}) &= \frac{\sin\bar{\theta}_s\sin\omega_s}{\cos\delta_s} \end{aligned} \tag{22}$$

We can also derive the position of the spin axis (ω_0, θ) with respect to the sun from

$$\begin{aligned} \cos\theta &= \sin\delta\sin\delta_s + \cos\delta\cos\delta_s\cos(\alpha_s - \alpha) \\ \sin\omega_0 &= \frac{\cos\delta_s\sin(\alpha_s - \alpha)}{\sin\theta} \end{aligned} \tag{23}$$

and the right ascensions and declinations of the diffuse (α_1, δ_1) and specular (α_2, δ_2) reflections from

$$\begin{aligned} \sin \delta_1 &= \sin \delta \cos (\theta + \epsilon) + \cos \delta \sin (\theta + \epsilon) \cos \omega_0 \\ \sin (\alpha_1 - \alpha) &= \frac{\sin (\theta + \epsilon) \sin \omega_0}{\cos \delta_1} \end{aligned} \tag{24}$$

$$\begin{aligned} \sin \delta_2 &= \sin \delta \cos (\theta + 2\epsilon) + \cos \delta \sin (\theta + 2\epsilon) \cos \omega_0 \\ \sin (\alpha_2 - \alpha) &= \frac{\sin (\theta + 2\epsilon)}{\cos \delta_2} \end{aligned} \tag{25}$$

The above equations have been derived for rotation about the major axis of the satellite. For rotation about a minor axis we replace θ with θ' and ϵ with $-\epsilon$ in Equations 24 and 25.

We are now in a position to determine ϕ_1 and ϕ_2 from

$$\cos \phi_1 = \sin \delta_0 \sin \delta_1 + \cos \delta_0 \cos \delta_1 \cos (\alpha_0 - \alpha_1) \tag{26}$$

$$\cos \phi_2 = \sin \delta_0 \sin \delta_2 + \cos \delta_0 \cos \delta_2 \cos (\alpha_0 - \alpha_2) \tag{27}$$

which, together with,

$$\cos \phi_0 = \sin \delta_0 \sin \delta + \cos \delta_0 \cos \delta \cos (\alpha_0 - \alpha) \tag{28}$$

enables equation 20 to be evaluated. Equations 20 through 28 therefore represent the perturbation to the semi-major axis due to incident, diffuse and specular radiation.

EXAMPLE

The magnitude and form of the perturbation can best be demonstrated by an example. Let us assume we have a circular orbit with inclination 90 degrees, and the sun on the equator. Because the shadow entry and exit points are symmetric about the Earth-sun line Equation 20 reduces to

$$\Delta a = -\frac{2}{n^2 m}\left[E_D \cos\phi_1 + E_s \cos\phi_2\right]_{\text{shadow exit}}^{\text{shadow entry}} \tag{29}$$

For this particular example it is preferable to use slightly different formulations for $\cos\phi_1$ and $\cos\phi_2$. Let ϕ_0' be the value of ϕ_0 at the point of entry and exit into the shadow, then we can write (see Figure 6)

$$\cos\phi_{1N} = \cos(\theta+\epsilon)\cos\phi_0' + \sin(\theta+\epsilon)\sin\phi_0'\cos(\omega_1+\omega_2) \tag{30}$$

$$\cos\phi_{1X} = \cos(\theta+\epsilon)\cos\phi_0' + \sin(\theta+\epsilon)\sin\phi_0'\cos\omega_1 \tag{31}$$

and

$$\cos\phi_{2N} = \cos(\theta+2\epsilon)\cos\phi_0' + \sin(\theta+2\epsilon)\sin\phi_0'\cos(\omega_1+\omega_2) \tag{32}$$

$$\cos \phi_{2X} = \cos (\theta + 2\epsilon) \cos \phi_0' + \sin (\theta + 2\epsilon) \sin \phi_0' \cos \omega_1 \qquad (33)$$

where $\phi_{1N}, \phi_{1X}, \phi_{2N}, \phi_{2N}$ are the shadow entry and exit values of ϕ_1 and ϕ_2. The angles ω_1 and ω_2 are defined in Figure 6.

We can now write

$$\Delta a = \frac{4}{n^2 m} \sin \phi_0' \sin \left(\omega_1 + \frac{\omega_2}{2}\right) \sin \frac{\omega_2}{2} \left[E_D \sin (\theta + \epsilon) + E_s \sin (\theta + 2\epsilon)\right] \qquad (34)$$

The $\sin \phi_0'$ term changes slowly as the orbit moves with respect to the sun but its sign is always positive. The $\sin \omega_2/2$ term is zero when there is no shadow on the orbit and the perturbation vanishes. When non-zero, the term is always positive. The term containing E_D and E_s changes only slowly as the spin axis moves and is normally of constant sign. However, for an oblate satellite the sine terms can change sign if $2\epsilon > \theta'$. The $\sin (\omega_1 + \omega_2/2)$ is also positive unless ω_1 is negative, implying that the spin axis lies near the equatorial plane and between the sun and the shadow points on the orbit.

Let us further simplify our example by having the precession axis on the equator, so that $\bar{\omega} = \pi/2$ on $\bar{\delta} = 0$, and let the spin axis rotate slowly about the precession axis. The $\sin (\omega_1 + \omega_2/2)$ term in equation 34 will then oscillate about zero with a period equal to the precession period and produce a quasi-periodic perturbation about the mean value. This situation could have existed for the Pageos satellite in July 1968. Reference 4 indicates that the spin axis of Pageos was near the equator on July 4th and if the axis was precessing about a point even nearer the equator we should expect to observe a quasi-periodic perturbation in the semi-major axis. The predicted maximum magnitude of this perturbation of Pageos, assuming a specular albedo of 0.86 (Reference 4) and negligible diffuse albedo, a mass of 55 kg, a mean motion of 8 revolutions/day is about 1 km/day or an acceleration of 8×10^{-4} revolutions/day^2 in mean anomaly. The observed amplitude of the acceleration shown in Figure 1 is about 1×10^{-4} revolutions/day^2. When account is taken of the trigonometric terms in equation 34 and of smoothing in the observational data; the amplitudes of the computed and observed perturbations are about equal.

CONCLUSIONS

Expressions have been developed for the perturbation of the semi-major axis of the orbit of a satellite with elliptical cross-section due to solar radiation pressure when both specular and diffuse reflections are taken into account. The theory has been applied to a very simplified example resembling the orbit of the Pageos satellite in July 1968 and it has been shown that if the spin axis is permitted to rotate about a fixed precession axis a perturbation of the semi-major axis is predicted which has approximately the same form and amplitude that is actually observed in the Pageos orbit.

The foregoing theory and example do not necessarily explain the perturbations in the Pageos and 1963-30D orbits but do suggest that a mechanism of the type described here could be the explanation. A more detailed examination of the theory and its application to these two satellites is being undertaken.

REFERENCES

1. Fea, K., "The Orbital Acceleration of High Balloon Satellites," presented at XIIth Plenary Meeting of COSPAR, Prague, May 1969.

2. Fea, Kenneth H. and Smith, David E. "Some Further Studies of Pertubation of Satellites at Great Altitude," accepted for Publication in Planetary and Space Science.

3. Vanderburgh, R. C., "Wide Band (Visual Spectrum) Photoelectric Photometry of PAGEOS During its First Fifteen Months in Orbit," Proceedings of University of Miami Symposium on Optical Properties of Orbiting Satellites, Edit. Duke, D., and Kissell, K. E., May 1969.

4. Vanderburgh, R. C., "ARL OPOS Photoelectric Photometry of PAGEOS on 4 July 1968," Aerospace Research Laboratories report ARL-MR-68-0004. Wright Patterson Air Force Base, Ohio, August 1968.

5. Smith, D. E., "An Approximate Method of Estimating the Reflection Characteristics of a Spherical Satellite," Proceedings of University of Miami Symposium on Optical Properties of Orbiting Satellites, Edit. Duke, D., and Kissell, K. E,, May 1969.

6. Cook, G. E., Geophys. J., Vol. 6, No. 3, April 1962.

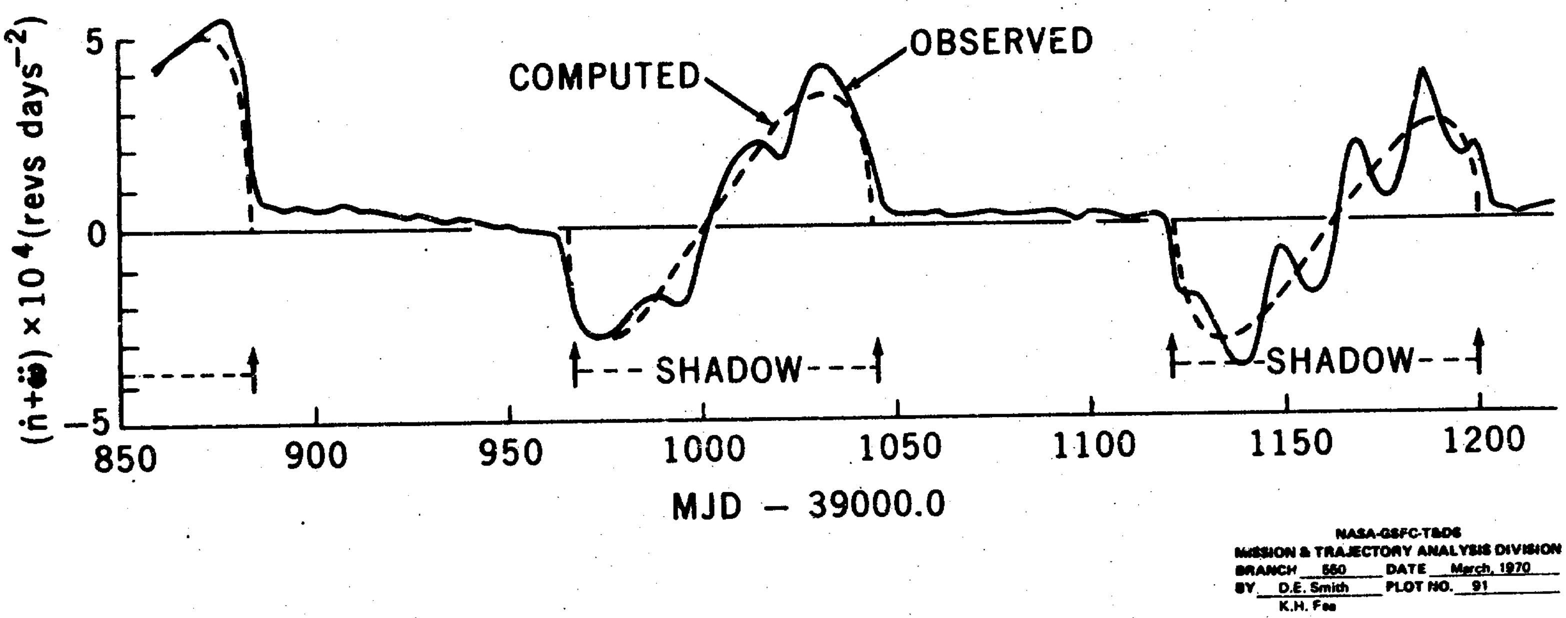

Figure 1. 1966 56A, Observed and Computed Orbital Acceleration v. Modified Julian Date (1968)
(after Fea, Reference 1)

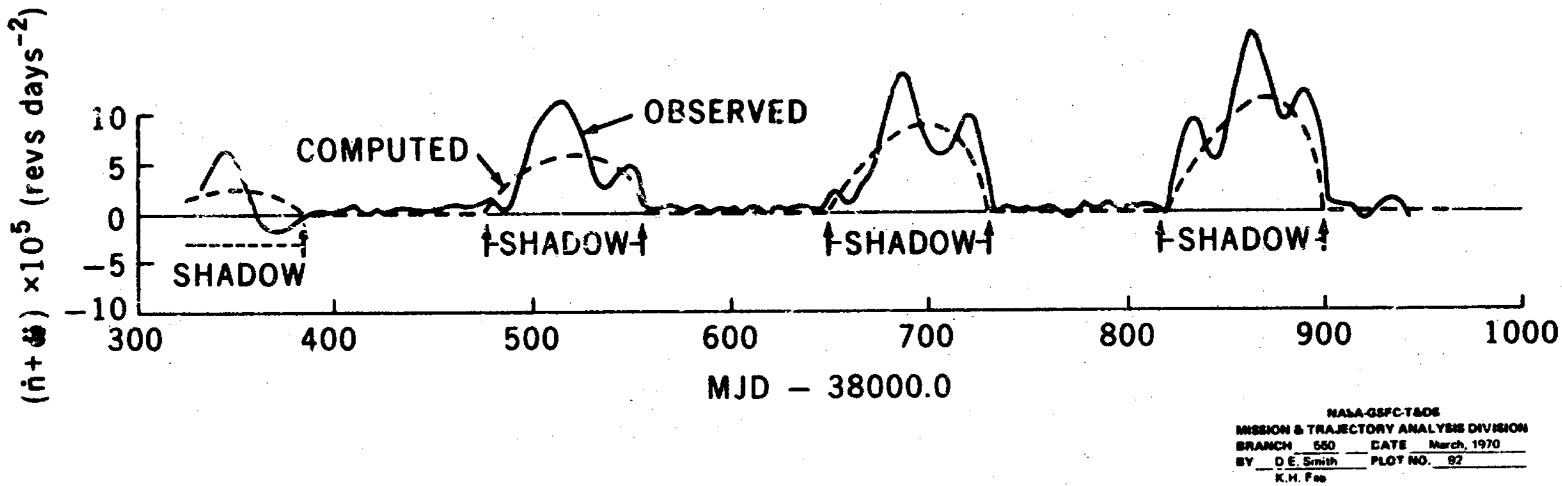

Figure 2. 1963 30D, Observed and Computed Orbital Acceleration v. Modified Julian Date (Nov. 1963 to Jun. 1965) (after Fea and Smith, Reference 2)

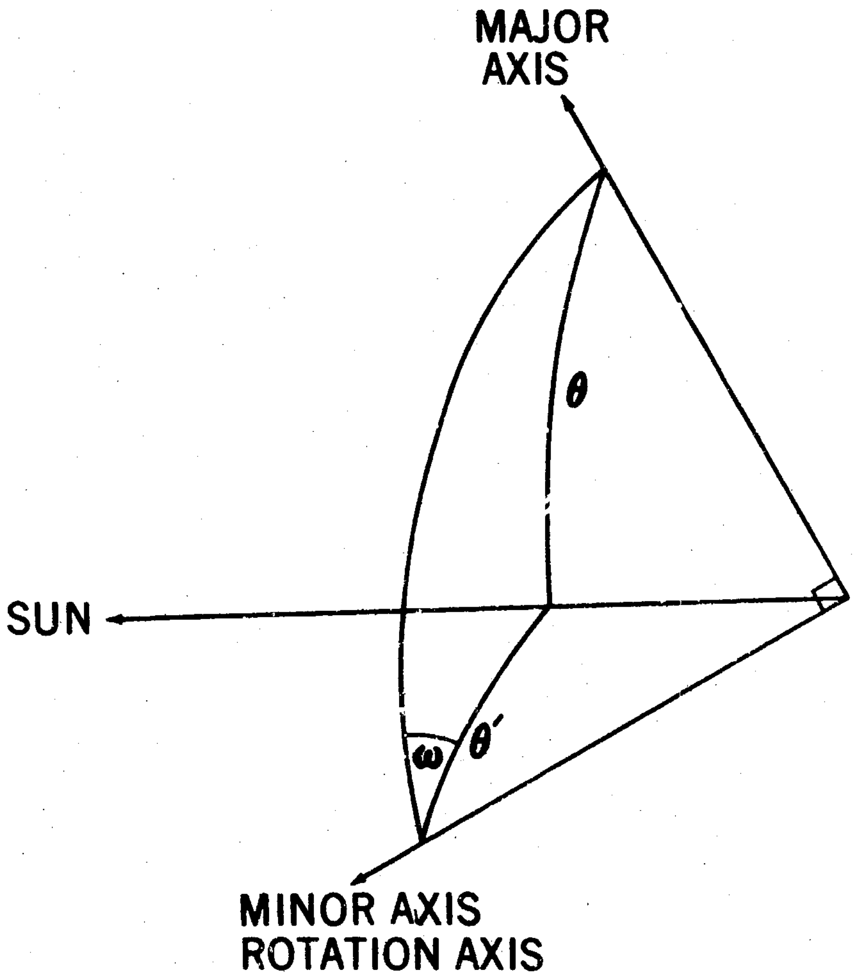

NASA-GSFC-T&DS
MISSION & TRAJECTORY ANALYSIS DIVISION
BRANCH 550 DATE March, 1970
BY D.E. Smith PLOT NO. 93
K.H. Fee

Figure 3. Rotation of Satellite About a Minor Axis.

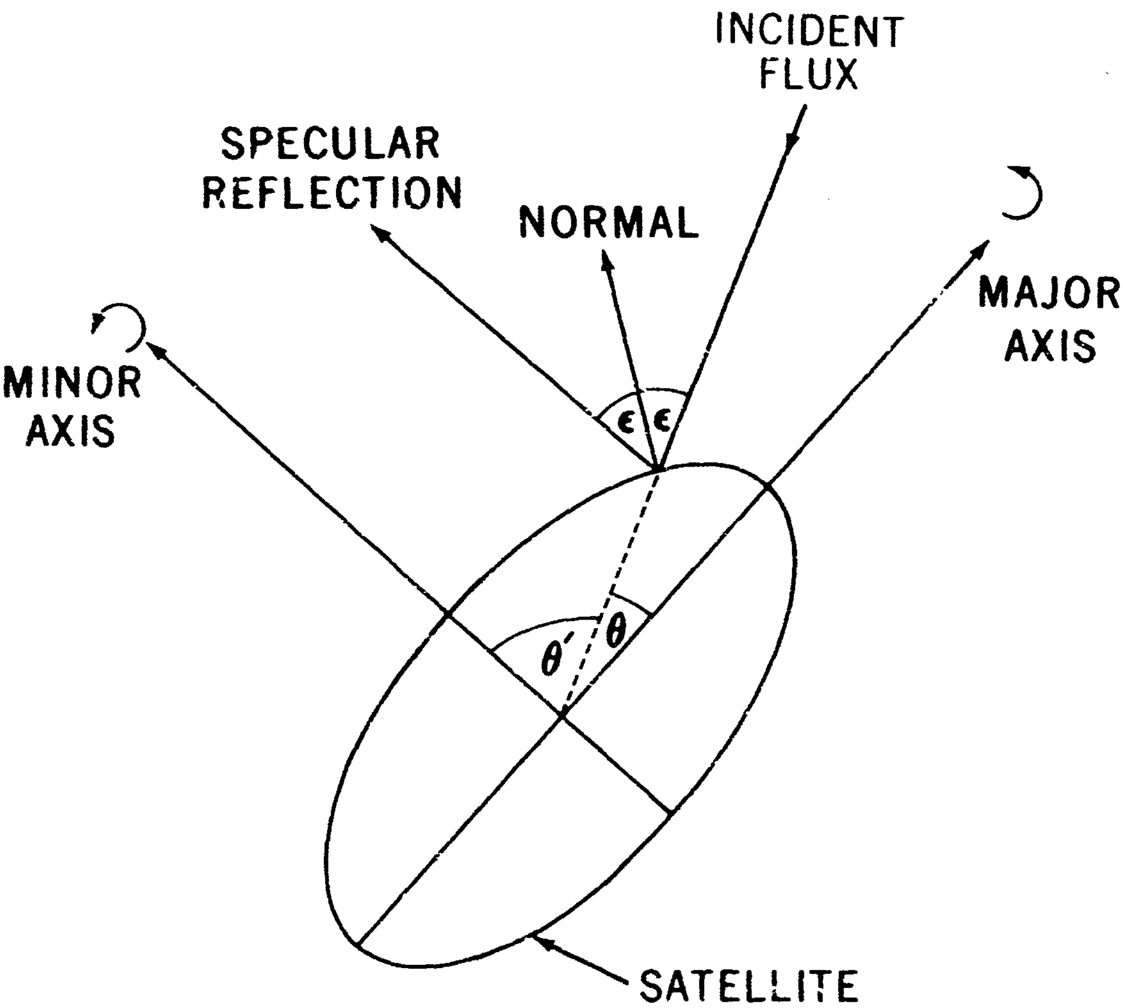

NASA-GSFC-T&DS
MISSION & TRAJECTORY ANALYSIS DIVISION
BRANCH 550 DATE March, 1970
BY D.E. Smith PLOT NO. 94
K.H. Fea

Figure 4. Incident and Reflected Radiation.

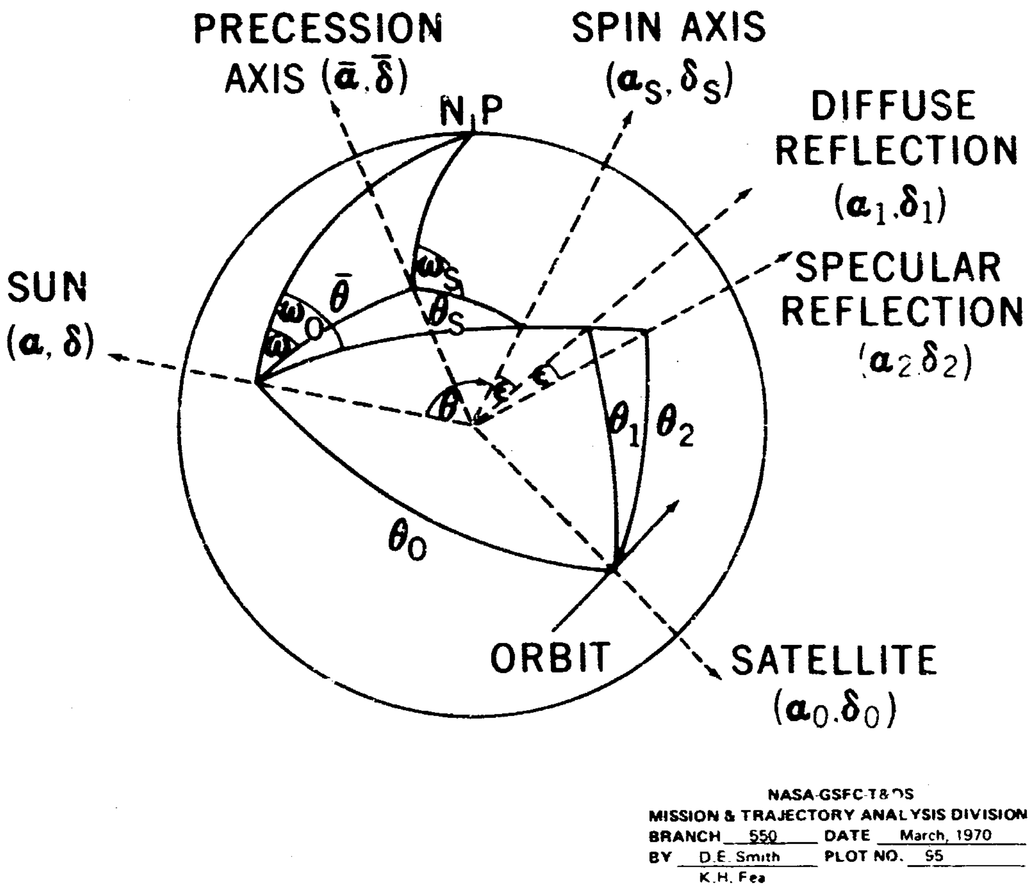

Figure 5. Relationship between Sun, Precession and Spin Axes, Diffuse and Specular Reflections, for Satellite Rotation about Major Axis.

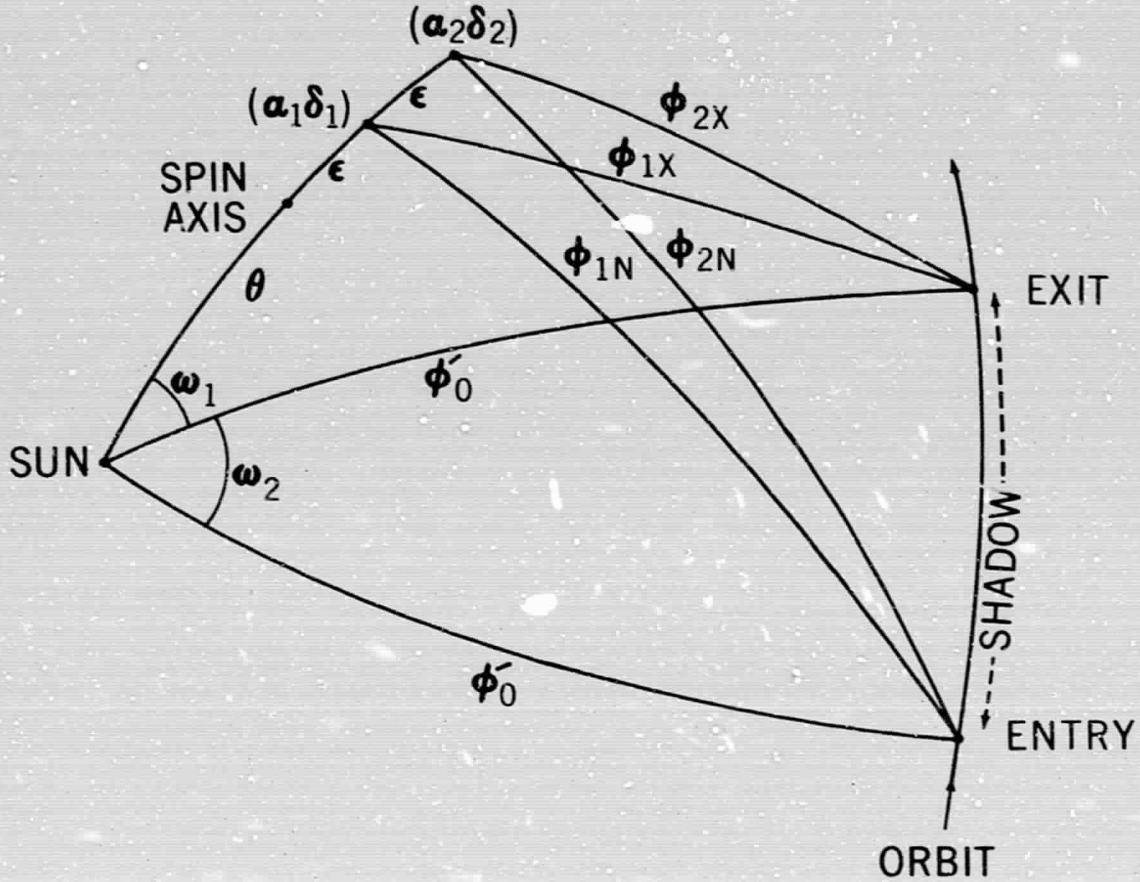

NASA-GSFC-T&DS
MISSION & TRAJECTORY ANALYSIS DIVISION
BRANCH 550 DATE March, 1970
BY D.E. Smith PLOT NO. 96
K.H. Fea

Figure 6. Shadow Entry and Exit Geometry for a Circular Orbit.